MerR-fluorescent protein chimera biosensor for fast and sensitive detection of Hg^{2+} in drinking water

Canan Özyurt[1,2]
Handan Üstükarcı[1]
Serap Evran[1*]
Azmi Telefoncu[1,3]

[1]Department of Biochemistry, Faculty of Science, Ege University, Bornova-Izmir, 35100, Turkey

[2]Department of Chemistry and Chemical Processing Technologies, Lapseki Vocational School, Canakkale Onsekiz Mart University, Canakkale, Lapseki, Turkey

[3]Bio-sensing and Bioinformatics Nanotechnologies R & D Trade & Ind. Ltd Co, TECHNOPARK EGE, Ege University, 35100, Izmir, Turkey

Abstract

Mercury ion (Hg^{2+}) is a universal pollutant and its detection is crucial for public healthcare. In this study, we developed a novel fluorescent biosensor by construction of a protein fusion between the mercury-sensing transcription factor MerR and enhanced yellow fluorescent protein (EYFP). Hg^{2+}-induced conformational change of MerR was transduced into fluorescence signal. Fluorescence intensity of the biosensor protein decreased with increasing concentrations of Hg^{2+} and a linear response was obtained in the range of 0.5–40 nM. The limit of detection was 0.5 nM, which was much lower than the maximum allowed level in water. The biosensor specificity was highly dependent on type and concentration of metal ion. The biosensor exhibited high specificity in a mixture of metal ions at 0.5 nM concentration. However, the interference effect was more pronounced at 40 nM concentration of metal ions. The measurement was completed in less than 1 Min with no need for sample preparation or preincubation steps. The biosensor achieved accurate and reliable detection in the spiked drinking water sample, as validated by the inductively coupled plasma optical emission spectrometry. Volume 66, Number 5, Pages 731–737, 2019

Keywords: *Hg^{2+}, fluorescent protein, mercury biosensor*

1. Introduction

Mercury (Hg) is a widespread environmental pollutant exhibiting toxicity on human neural and internal secretion systems [1, 2]. Hg in the environment exists in elemental, inorganic, and organic forms. Elemental Hg (Hg0) is slightly water soluble, whereas inorganic Hg ion (Hg^{2+}) is more water soluble and readily absorbed by gastrointestinal tract [3, 4]. Contaminated drinking water is the major source of exposure to heavy metals [5]. Therefore, the most frequently analyzed material is water samples [6]. According to the United States Environmental Protection Agency (US EPA) standards, the maximum allowable level of Hg in drinking water is 10 nM [7]. Cold vapor atomic absorption spectrometry [8, 9], inductively coupled plasma mass spectrometry [10–12], and cold vapor atomic fluorescence spectroscopy [13, 14] are the commonly used methods for Hg analysis. However, novel methods enabling shorter analysis time, direct sample analysis, and low instrumentation costs are needed. As reviewed elsewhere [15, 16], several fluorescent, colorimetric, and electrochemical biosensors were constructed for Hg detection. Hg-specific oligonucleotides [17, 18], peptide nucleic acid [19], specific monoclonal antibody [20], and

Abbreviations: *Ag^{+}, silver ion; Cd^{2+}, cadmium ion; Cu^{2+}, copper ion; EYFP, enhanced yellow fluorescent protein; Fe^{2+}, ferrous iron; GFP, green fluorescent protein; Hg^{2+}, mercury ion; ICP-OES, inductively coupled plasma optical emission spectrometry; IPTG, isopropyl-β-D-thiogalactopyranoside; MerR, Mercury-sensing transcription factor; Mg^{2+}, magnesium ion; Mn^{2+}, manganese ion; Ni^{2+}, nickel ion; Pb^{2+}, lead ion; Zn^{2+}, zinc ion.*

**Address for correspondence: Serap Evran, PhD, Department of Biochemistry, Faculty of Science, Ege University, Bornova-Izmir35100, Turkey. Tel.: +90 2323112304; Fax: +90 232 3115485; e-mail: serap.evran@ege.edu.tr.*

[Correction added on 17 October 2019, after first online publication: Azmi Telefoncu's affiliations were amended.]

Additional supporting information may be found online in the Supporting Information section at the end of the article.

Received 22 May 2019; accepted 12 August 2019

DOI: 10.1002/bab.1805

Published online 30 August 2019 in Wiley Online Library (wileyonlinelibrary.com)

metallothionein [21] were used as biorecognition components of Hg biosensors.

Discovery of green fluorescent protein (GFP) [22] and development of color-shifted GFP variants [23] enabled researchers to design genetically encoded fluorescent protein-based biosensors [24, 25]. Autofluorescent property, a unique chromophore hidden in the β-barrel scaffold, high stability and small size are some superior features of GFP family proteins [26, 27]. Genetically encoded fluorescent biosensors are powerful tools to monitor heavy metals [28]. Two classes of biosensors can be designed for this purpose: (i) single fluorescent protein-based biosensors and (ii) conformation-based biosensors. Single fluorescent protein-based biosensors rely on the intrinsic fluorescence change in GFP or its engineered variants. There are successful examples of single fluorescent protein-based metal biosensors. For instance, the GFP mutant harboring two cysteines at positions 145 and 205 showed a fluorescence quenching in the presence of micromolar concentrations of Pb^{2+} [29]. A similar fluorescence quenching-based Hg^{2+} biosensor was obtained by introducing cysteine residue at position 205 of GFP [30]. The histidine to cysteine mutation at position 148 created a GFP variant with enhanced fluorescence response upon addition of Hg^{2+} [31]. Blocking of the chromophore conjugation by Hg^{2+} provided a turn-off infrared fluorescent protein probe [32]. Metal-binding site was engineered into flavin-binding fluorescent protein to obtain a probe for Hg^{2+} [33]. A novel Hg^{2+} sensor was developed by genetic incorporation of unnatural amino acid into the chromophore of circularly permutated GFP [34].

Conformation-based single fluorescent protein sensors are different in that a specific ligand binding domain is attached or inserted into the fluorescent protein. Ligand-induced conformational change is transduced into fluorescence signal, which is sensitive to chromophore local environment. The copper regulatory protein Ace1 was inserted into yellow fluorescent protein (EYFP), and the fusion protein was used as a fluorescent reporter for Cu^{+} [35]. Similarly, Zn^{2+} sensor was designed by attaching the Zn^{2+} binding domain of Zap1 transcription factor to the circularly permutated GFP [36].

MerR is the Hg-sensing transcription factor that regulates expression of detoxification genes [37–39]. Upon Hg^{2+} binding, MerR undergoes extensive conformational changes that lead to the assembly of Hg^{2+} binding site. Conformational repositioning of three Hg^{2+}-ligating cysteine residues provides the selectivity for Hg^{2+} [40]. The selective binding property of MerR was used to design fluorescent biosensor [41], as well as surface plasmon resonance sensor that could monitor Hg^{2+}-induced dissociation of MerR from DNA [42]. MerR was immobilized onto gold electrode and the capacitance change was monitored at different concentrations of Hg^{2+} [43].

In this study, we report the first conformation-based fluorescent protein biosensor for simple, fast, and sensitive detection of Hg^{2+}. We attached MerR to the N-terminal of EYFP and obtained MerR:EYFP chimera biosensor. The purified biosensor protein was successfully applied to detect Hg^{2+} in drinking water, as validated by the inductively coupled plasma optical emission spectrometry (ICP-OES). The biosensor was characterized in terms of detection limit, linear range, specificity, and accuracy.

2. Materials and Methods

2.1. Materials

Isopropyl-β-D-thiogalactopyranoside (IPTG), Taq DNA polymerase, DNA ligase, and Pierce Unstained Protein MW Marker were purchased from ThermoScientific (Rockford, IL, USA). Restriction enzymes were purchased from New England Biolabs (Beverly, MA, USA). HisTrap FF crude column (5 mL) was purchased from GE Healthcare (Chicago, IL, USA). Oligonucleotide primers for PCR were obtained from Metabion International AG (Martinsried, Germany). All other chemicals were of analytical grade and purchased from Sigma–Aldrich (St. Louis, MO, USA) or Carl Roth GmbH (Karlsruhe, Germany). The plasmid encoding EYFP was a kind gift from Prof. Dr. Constantinos E. Vorgias from National & Kapodistrian University of Athens.

2.2. Construction of the plasmid encoding MerR:EYFP chimera protein

In order to generate MerR:EYFP construct, the two gene fragments were fused by using overlap extension PCR [44]. Fusion PCR was achieved in three separate rounds with the specific primers given in Supp. Table S1. The overlapping primers 3 and 4 included a DNA sequence encoding 5-amino acid linker (GGSGG) [45]. In the first round, the gene encoding MerR (GenBank: AP008226.1) was amplified from genomic DNA of *Thermus thermophilus* HB8 by using primers 1 and 3. In the second round, the gene encoding EYFP was amplified from the plasmid by using primers 2 and 4. In the final PCR round, the gel-purified fragments were fused by using primers 1 and 2. Fusion PCR was performed as follows: 95 °C for 3 Min; 30 cycles of 95 °C for 45 Sec, 58 °C for 45 Sec, and 72 °C for 1 Min 15 Sec; followed by a final extension for 10 Min. The fusion PCR product was cloned between *Not*I and *Xho*I restriction sites of pET21a(+) vector (Novagen, Madison, WI, USA).

2.3. Recombinant production and purification of the biosensor protein

The plasmid encoding MerR:EYFP biosensor protein was transformed into chemically competent *Escherichia coli* T7-Rosetta cells (Novagen). Protein expression was induced by 0.5 mM IPTG at 20 °C. Following incubation under dark conditions for 18 H at 200 rpm, the cells were harvested and resuspended in 50 mM potassium phosphate buffer containing 300 mM NaCl and 5 mM imidazole (pH 7.8). The cells were homogenized using ultrasonic homogenizer VCX 500 (Sonics & Materials, Inc., Newtown, CT, USA). The biosensor protein was purified using the HisTrapFF crude column connected to ÄKTAprime plus chromatography system (GE Healthcare). Protein concentration was determined by Bradford's method [46], and the purity was monitored by SDS-PAGE in 12.5% gel [47]. The purified

protein was stored in 50 mM potassium phosphate buffer (pH 7.8) containing 300 mM NaCl and 5 mM imidazole. Immediately before fluorescence measurements, buffer exchange in 50 mM HEPES pH 7.5 containing 150 mM NaCl was performed by ultrafiltration (Amicon Ultra-15 Centrifugal Filter Units, 10000 NMWL; Merck Millipore, Darmstadt, Germany).

2.4. Fluorescence measurements for Hg^{2+} detection

Fluorescence measurements were performed with Cary Eclipse spectrofluorimeter (Agilent Technologies, California, CA, USA) equipped with magnetic stirrer and temperature control unit. All solutions were freshly prepared with ultra-pure water (18 MΩ) and filtered through 0.22 μM syringe filter. Biosensor protein (0.1 mg) was added to 2 mL of 50 mM HEPES buffer (pH 7.5) in a 2-mL quartz cuvette of 1-cm path length. Increasing concentrations of Hg^{2+} (0–40 nM) were added to the cuvette, and the change in fluorescence intensity was immediately measured without further incubation. Fluorescence emission at 527 nm was monitored at the excitation wavelength of 512 nm. The excitation and the emission slits were set at 5 nm. All measurements were performed at 25 °C.

In order to investigate the interference of other metal ions, the measurements were performed with Mg^{2+}, Fe^{2+}, Ag^{+}, Ni^{2+}, Cu^{2+}, Zn^{2+}, Mn^{2+}, Pb^{2+}, Cd^{2+} separately, or the mixture of them.

2.5. Sample analysis

The bottled drinking water was obtained from a local market. The water sample was centrifuged at 10,060 g for 10 Min and filtered through 0.22 μM syringe filter. $HgCl_2$ solution was prepared in 50 mM HEPES buffer (pH 7.0) and the water sample was spiked with $HgCl_2$ solution to reach the desired final concentration. Fluorescence measurements were performed as described above and the recovery percentage was calculated. In order to validate the biosensor performance, the water sample was spiked with 40 nM Hg^{2+} and analyzed by standard ICP-OES. ICP-OES analysis was performed according to the EPA method 6010C using ICP-OES Optima 7000 DV (PerkinElmer, Waltham, MA, USA) at Dokuz Eylul University, Turkey.

3. Results and Discussion

3.1. Purification of the biosensor protein

The biosensor protein was constructed by fusing MerR to the N-terminal of EYFP, and then expressed in *E. coli* cells. SDS-PAGE analysis showed that the His-tagged MerR:EYFP biosensor protein was obtained with high purity (>90%) and appeared at the expected molecular weight of ~45 kDa (Supp. Fig. S1). Purification yield of the overexpressed MerR:EYFP biosensor protein was 30 mg per 1 L of culture.

3.2. Sensitivity of the biosensor

We constructed a protein chimera biosensor employing MerR protein as the Hg^{2+} sensing element and EYFP as the fluorescent reporter. The peptide linker was inserted between fusion partners in order to enhance flexibility and provide rotational

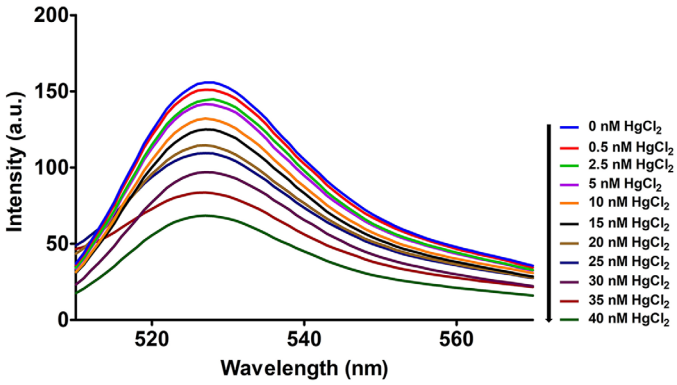

FIG. 1 *The change in fluorescence intensity upon treatment of the purified MerR:EYFP protein with increasing concentrations of $HgCl_2$.*

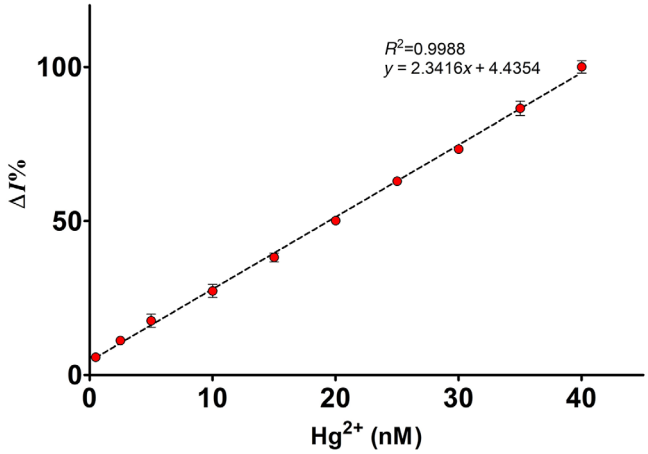

FIG. 2 *Plot of the %change in fluorescence intensity with increasing concentrations of Hg^{2+} in the range of 0.5–40 nM.*

freedom between MerR and EYFP. As revealed by molecular dynamics studies [48], Hg^{2+} induces conformational change in MerR. Thus, the detection strategy was based on transducing Hg^{2+} binding and conformational change events into a fluorescence signal. Treatment of MerR:EYFP chimera biosensor with increasing concentrations of Hg^{2+} caused a decrease in fluorescence intensity (Fig. 1). The percentage change in fluorescence intensity was calculated as $\Delta I = 100 \times (I_0 - I)/I_0$, where I_0 and I representing the fluorescence intensity before and after addition of Hg^{2+}, respectively. The fluorescence change was plotted against the concentration of Hg^{2+}. As shown in Fig. 2, a linear detection range of 0.5–40 nM was obtained. When the biosensor protein was incubated with higher Hg^{2+} concentrations in the range of 40–200 nM, the saturation in the biosensor response was observed (Supp. Fig. S2). The biosensor achieved high sensitivity with a limit of detection (LOD) of 0.5 nM, which was 20-fold lower than the US EPA limit in drinking water.

To ensure that the decrease in fluorescence intensity is not related to self-quenching of the fluorescence protein, EYFP

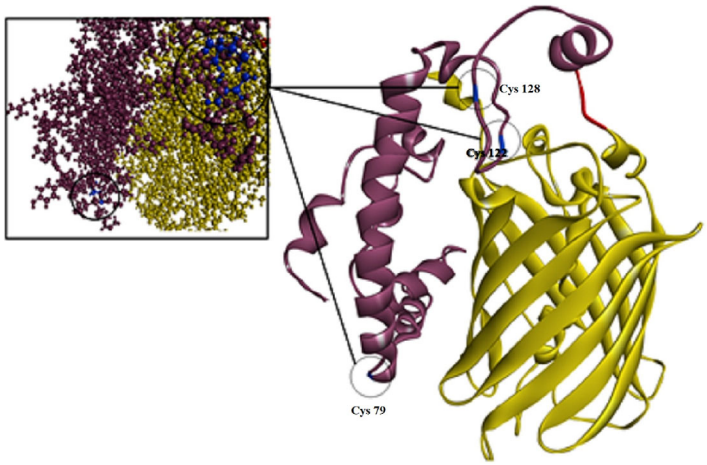

FIG. 3 *Three-dimensional structure of MerR:EYFP protein chimera predicted by I-TASSER. The three cysteine residues (Cys 79, Cys 122, and Cys 128), which assembly a specific binding site for Hg^{2+} are indicated in blue color.*

was similarly treated with increasing concentrations of Hg^{2+}. For this aim, EYFP was cloned, produced and purified from *E. coli* as described for recombinant production of MerR:EYFP. As shown in Supp. Fig. S3, no significant fluorescence change was observed upon treatment of EYFP with Hg^{2+} in the concentration range of 0.5–40 nM. This finding supports that the three coordinated cysteine residues of MerR form the main binding element of MerR:EYFP chimera biosensor. Thus, Hg^{2}-induced conformational change is responsible for local environmental change around the chromophore of EYFP. For further confirmation, I-TASSER (Iterative Threading ASSEmbly Refinement) protein modeling program [49] was used to predict the three dimensional structure of MerR:EYFP protein chimera. The *C*-score indicates confidence of the predicted model and should be between −5 and 2 values. Accordingly, the *C*-score of the predicted model of MerR:EYFP was −2.17. As shown in Fig. 3, the predicted model revealed the presence of characteristic β-barrel structure surrounding the fluorophore, as well as the three accessible Hg^{2+}-ligating cysteine residues. The predicted protein structure supports the experimental results obtained from fluorescence measurements.

As summarized in Table 1, MerR:EYFP chimera biosensor showed higher sensitivity when compared with four of the previously reported single fluorescent protein biosensors [30–34]. Although the LOD values of GFP mutant biosensor [31] and MerR:EYFP chimera biosensor were same, the highest detectable Hg^{2+} concentration was more than 10-fold higher for MerR:EYFP. Metal-binding peptides have also been used to design Hg sensors, albeit with a lower sensitivity than MerR:EYFP chimera biosensor. Incorporation of two pyrene (Py) fluorophores into the tetrapeptide has allowed a detection limit of 31.2 nM [51]. A complex between the peptide dH3w and Zn^{2+} has been used as a probe with a detection limit of 56 nM [52].

TABLE 1 *Comparison of linear range and detection limits (LOD) of single fluorescent protein-based Hg^{2+} biosensors*

Biosensor construct	*Linear range*	*LOD*	*Reference*
GFP mutant	n.d.	~2 nM	[30]
GFP mutant	0.5–3.0 nM	0.5 nM	[31]
Infrared fluorescent protein (IFP)	0–300 nM and 600–2400 nM	<50 nM	[32]
Flavin-binding fluorescent protein (FbFP) mutant	0.1–3.0 μM	0.1 μM	[33]
Circularly permuted GFP variant	n.d.	0.8 μM	[34]
MerR:EYFP protein chimera	0.5–40 nM	0.5 nM	This study

The results showed that construction of a chimera of MerR and EYFP was a successful strategy to improve detection properties. To the best of our knowledge, MerR:EYFP chimera biosensor is the first conformation-based fluorescent protein biosensor for detection of Hg^{2}. Single fluorescent protein biosensor response relies on direct interaction between analyte and chromophore of fluorescent protein. For this purpose, fluorescent protein mutants need to be produced by protein design [53]. Conformation-based biosensors provide more versatility than fluorescent protein variants, as various ligand binding proteins can be simply attached to fluorescent proteins [54]. Moreover, combination of natural ligand binding proteins with fluorescent proteins allows large dynamic range [55]. In consistent with this study, we similarly obtained a larger dynamic range compared with that of GFP mutant [31].

During fluorescence measurements, the concentration of the biosensor protein was adjusted to 0.05 mg/mL. When the biosensor concentration was above 0.05 mg/mL, the fluorescence was over range and interfered with the measurement. At protein concentrations below 0.05 mg/mL, early saturation was observed and a very narrow dynamic range was obtained.

The principle of MerR:EYFP chimera biosensor is based on conformational change of MerR and monitoring the fluorescence quenching of EYFP. MerR was used as the sensing component because of its well-characterized conformational switch [40]. As explained elsewhere [24], ligand binding to the sensing protein domain is communicated to the fluorescent protein as a local distortion in its structure. As a result of structural distortion, the fluorescence can be quenched or the equilibrium between the protonated and unprotonated forms of the chromophore can be altered.

3.3. Specificity of the biosensor

To validate the specificity of the biosensor, fluorescence measurements were performed in the presence of nine potential interfering metal ions. As shown in Fig. 4 and Supp. Table

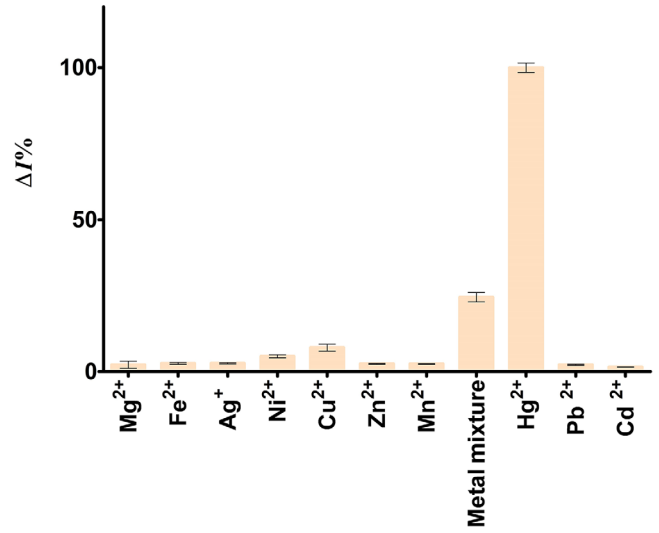

FIG. 4 *Interference effect of different metal ions on the biosensor response. MerR:EYFP biosensor protein was treated with 0.5 nM of Mg^{2+}, Fe^{2+}, Ag^{+}, Ni^{2+}, Cu^{2+}, Zn^{2+}, Mn^{2+}, Pb^{2+}, and Cd^{2+} . The fluorescence signal was compared with the signal obtained for 0.5 nM Hg^{2+}.*

S2, MerR:EYFP biosensor exhibited a 12-fold higher response to Hg^{2+} compared with the nearest competitor Cu^{2+}. When a mixture of all interfering metal ions was used, the response to Hg^{2+} was still fourfold higher. The response to 0.5 nM of Mg^{2+}, Fe^{2+}, Ag^{+}, Ni^{2+}, Zn^{2+}, Mn^{2+}, Pb^{2+}, and Cd^{2+} was negligible. When the biosensor protein was treated with double mixtures of 0.5 nM Hg^{2+} and each interfering metal ion, a significant interference effect of $Ni^{2+,}$ Cu^{2+}, Zn^{2+}, and Pb^{2+} was observed (Supp. Fig. S4).

The specificity of the biosensor was also tested against 40 nM of interfering metal ions. As shown in Supp. Fig. S5 and Supp. Table S3, the biosensor could generate the highest response against Hg^{2+}. However, the interference effect was more pronounced.

The observed interference effect of other metal ions could be attributed to the presence of metal-binding His-tag, which was used for purification of MerR:EYFP protein. As observed before [56], the His-tag may bring metal ions closer to chromophore and cause quenching. As studied extensively [57–59], the complexes between histidine and metal ions have different characteristics. In case of MerR:EYFP, we observed different interference effects depending on the metal ion type and concentration. For instance, double mixture of 0.5 nM of Zn^{2+} and Hg^{2+} resulted in the highest response compared with that of 0.5 nM Hg^{2+} (Supp. Fig. S4). However, the biosensor response to 40 nM Zn^{2+} was about fourfold lower compared with Hg^{2+} (Supp. Fig. S5 and Supp. Table S3). In contrast, Ni^{2+} had a significant interference effect in both cases. Interestingly, MerR:EYFP biosensor exhibited almost the same response against 0.5 nM Hg^{2+} when the biosensor was tested in the presence of 0.5 nM of all interfering metal ions (Supp. Fig. S4).

TABLE 2 *Determination of Hg^{2+} in spiked drinking water sample*

Spiked (nM)	*Found (nM)*	*RSD (%) (n = 5)*	*Recovery (%) (n = 5)*
0.50	0.53	2.5	105.8
10.0	10.2	5.2	101.5
20.0	22.7	0.4	113.5
35.0	35.7	2.5	101.9
40.0	40.8	2.8	102.0

The results showed that MerR:EYFP biosensor was highly specific to Hg^{2+} over other competing ions at 0.5 nM concentration. The specificity of the biosensor can be attributed to three cysteines residues of MerR, which assembly a specific binding site and a rare trigonal coordination environment for Hg^{2+} [40, 50]. However, the His-tag on the specificity of the biosensor should also be considered.

3.4. Analytical performance

Drinking water was spiked with Hg^{2+} at a concentration range of 0.5–40 nM. The fluorescence response of MerR:EYFP biosensor was measured and Hg^{2+} concentration was calculated according to the standard curve equation: $y = 2.3416x + 4.4354$. As shown in Table 2, the recovery values ranged from 101.5% to 113.5%, and the relative standard deviations (RSD%, $n = 5$) were in the range of 0.4–5.2. Although the results indicate that MerR:EYFP biosensor is promising for real water sample analysis with good reproducibility and reliability, the biosensor performance should also be tested in industrial water samples with high concentrations of ions and organic substances. A whole-cell bacterial biosensor using GFP gene as the reporter has been previously reported [60]. MerR:EYFP biosensor should also be compared with whole-cell Hg biosensors for use in environmental samples.

3.5. Stability of the biosensor

As the biosensor is a fluorescent protein fusion of MerR, its stability could be affected by several factors. As shown before [61], storage stability depends on relative position of fluorescent protein and fusion partner, linker length and design. In case of MerR:EYFP fusion, we could not detect the Hg^{2+}-induced fluorescence signal change after incubation of the biosensor protein at 4 °C for 2 weeks (data not shown). Detailed biophysical characterization as well as further protein design studies are needed to optimize the stability of MerR:EYFP biosensor.

3.6. Validation of the biosensor by ICP-OES

The reliability of MerR:EYFP biosensor was further evaluated by comparison with a standard method. For this aim, drinking water was spiked with 40 nM Hg^{2+} and analyzed by ICP-OES. For comparison, the same sample was treated with MerR:EYFP

TABLE 3 *Comparison of analysis results obtained by MerR:EYFP biosensor and inductively coupled plasma optical emission spectrometry (ICP-OES)*

Sample	*Found by MerR:EYFP chimera biosensor*	*Found by ICP-OES*
Drinking water spiked with 40 nM Hg^{2+}	40.8 ± 2.8 nM	40.0 ± 0.5 nM

biosensor, and Hg^{2+} concentration was calculated according to the standard curve. As shown in Table 3, the developed biosensor provided a reliable result that was comparable to that obtained by ICP-OES.

4. Conclusions

We developed a novel genetically encoded fluorescent biosensor for Hg^{2+}, which was constructed by fusing a specific Hg^{2+}-binding protein (MerR) and fluorescent protein (EYFP). The biosensor achieved subnanomolar sensitivity (0.5 nM), which was 20-fold lower than the maximum acceptable limit. High specificity over 0.5 nM of other metal ions was achieved by using MerR, a highly specific protein that undergoes conformational changes to assembly the Hg^{2+} binding site. As indicated by specificity tests, further studies are needed to explain the differences in interference of other metal ions. The His-tag could be removed to enhance the specificity at higher concentrations of metal ions. Compared with ICP-OES and other standard methods requiring sample preparation, the developed MerR:EYFP biosensor allowed direct sample analysis. Moreover, the biosensor provided a very short analysis time (less than 1 Min). Matrix effect was evaluated by testing the biosensor in drinking water samples. The good recovery percentage of the spiked samples indicated low susceptibility to matrix effect. The biosensor exhibited good recovery percentage and reliability, as validated by the ICP-OES method. Thus, MerR:EYFP biosensor shows potential as a simple and sensitive tool for monitoring Hg^{2+} in real water samples. Future structural studies would be helpful to reveal the mechanism of conformational change and biosensor response of MerR:EYFP chimera.

5. Acknowledgement

We thank Ege University Scientific Research Projects Coordination Unit for the financial support (project number: 2011 FEN 035).

The authors declare no conflict of interest.

6. References

[1] Jan, A., Azam, M., Siddiqui, K., Ali, A., Choi, I., Haq, Q. M. (2015) Int. J. Mol. Sci. 16, 29592–29630.
[2] Bjørklund, G., Dadar, M., Mutter, J., Aaseth, J. (2017) Environ. Res. 159, 545–554.
[3] Park, J. D., Zheng, W. (2012) J. Prev. Med. Public Health 45, 344–352.
[4] Zhu, S., Zhang, Z., Žagar, D. (2018) Sci. Total Environ. 639, 538–549.
[5] Rehman, K., Fatima, F., Waheed, I., Akash, M. S. H. (2018) J. Cell. Biochem. 119, 157–184.
[6] Suvarapu, L. N., Baek, S. O. (2017) Int. J. Anal. Chem. 2017, 3624015.
[7] US EPA. (2009) National Primary Drinking Water Regulations, Environmental Protection Agency (US) Washington, DC.
[8] Tuzen, M., Karaman, I., Citak, D., Soylak, M. (2009) Food Chem. Toxicol. 47, 1648–1652.
[9] Krawczyk, M., Stanisz, E. (2016) Talanta 161, 384–391.
[10] Ma, S., He, M., Chen, B., Deng, W., Zheng, Q., Hu, B. (2016) Talanta 146, 93–99.
[11] Zhu, S., Chen, B., He, M., Huang, T., Hu, B. (2017) Talanta 171, 213–219.
[12] Peng, C., He, M., Chen, B., Huang, L., Hu, B. (2017) Analyst 142, 4570–4579.
[13] Ebdon, L., Foulkes, M. E., Le Roux, S., Muñoz-Olivas, R. (2002) Analyst 127, 1108–1114.
[14] Amde, M., Liu, J.-F., Tan, Z. Q., Bekana, D. (2016) Talanta 149, 341–346.
[15] Chen, G., Guo, Z., Zeng, G., Tang, L. (2015) Analyst 140, 5400–5443.
[16] Bansod, B., Kumar, T., Thakur, R., Rana, S., Singh, I. (2017) Biosens. Bioelectron. 94, 443–455.
[17] Huang, R.-F., Liu, H.-X., Gai, Q.-Q., Liu, G.-J., Wei, Z. (2015) Biosens. Bioelectron. 71, 194–199.
[18] Wu, Z., Shen, H., Hu, J., Fu, Q., Yao, C., Yu, S., Xiao, W., Tang, Y. (2017) Anal. Bioanal. Chem. 409, 5209–5216.
[19] Bala, A., Górski, Ł. (2018) Bioelectrochemistry 119, 189–195.
[20] Xing, C., Liu, L., Zhang, X., Kuang, H., Xu, C. (2014) Anal. Methods 6, 6247–6253.
[21] Irvine, G., Tan, S., Stillman, M.J. (2017) Biosensors 7, 14.
[22] Tsien, R. Y. (1998) Annu. Rev. Biochem. 67,509-44.
[23] Day, R. N., Davidson, M. W. (2009) Chem. Soc. Rev. 38, 2887–2921.
[24] Frommer, W. B., Davidson, M. W., Campbell, R. E. (2009) Chem. Soc. Rev. 38, 2833–2841.
[25] Sanford, L., Palmer, A. (2017) Methods Enzymol. 589, 1–49.
[26] Stepanenko, O. V., Verkhusha, V. V., Kuznetsova, I. M., Uversky, V. N., Turoverov, K. K. (2008) Curr. Protein Pept. Sci. 9, 338–369.
[27] Stepanenko, O. V., Stepanenko, O. V., Kuznetsova, I. M., Verkhusha, V. V., Turoverov, K. K., (2013) Int. Rev. Cell Mol. Biol. 302, 221–278.
[28] Hao, Z., Zhu, R., Chen, P. R. (2018) Curr. Opin. Chem. Biol. 43, 87–96.
[29] Nadarajan, S. P., Ravikumar, Y., Deepankumar, K., Lee, C.-S., Yun, H. (2014) Chem. Commun. 50, 15979–15982.
[30] Chapleau, R. R., Blomberg, R., Ford, P. C., Sagermann, M. (2008) Protein Sci. 17, 614–622.
[31] Jiang, T., Guo, D., Wang, Q., Wu, X., Li, Z., Zheng, Z., Yin, B., Xia, L., Tang, J., Luo, W., Xia, N., Jiang, Y. (2015) Anal. Chim. Acta 876, 77–82.
[32] Gu, Z., Zhao, M., Sheng, Y., Bentolila, L. A., Tang, Y. (2011) Anal. Chem. 83, 2324–2329.
[33] Ravikumar, Y., Nadarajan, S. P., Lee, C.-S., Jung, S., Bae, D.H., Yun, H. (2016) J. Microbiol. Biotechnol. 26, 530–539.
[34] Shang, X., Wang, N., Cerny, R., Niu, W., Guo, J. (2017) ACS Sens. 2, 961–966.
[35] Liu, J., Karpus, J., Wegner, S. V., Chen, P. R., He, C. (2013) J. Am. Chem. Soc. 135, 3144–3149.
[36] Qin, Y., Sammond, D. W., Braselmann, E., Carpenter, M. C., Palmer, A. E. (2016) ACS Chem. Biol. 11, 2744–2751.
[37] Brown, N. L., Stoyanov, J. V., Kidd, S. P., Hobman, J. L. (2003) FEMS Microbiol. Rev. 27, 145–163.
[38] Giedroc, D. P., Arunkumar, A. I. (2007) Dalton Trans. 29, 3107–3120.
[39] Chen, P. R., He, C. (2008) Curr. Opin. Chem. Biol. 12, 214–221.
[40] Chang, C. C., Lin, L. Y., Zou, X. W., Huang, C. C., Chan, N. L. (2015) Nucleic Acids Res. 43, 7612–7623.
[41] Chen, P., He, C. (2004) J. Am. Chem. Soc. 126, 728–729.
[42] Taniguchi, M., Siddiki, M. S. R., Ueda, S., Maeda, I. (2015) Biosens. Bioelectron. 67, 309–314.
[43] Bontidean, I., Lloyd, J. R., Hobman, J. L., Wilson, J. R., Csöregi, E., Mattiasson, B., Brown, N. L. (2000) J. Inorg. Biochem. 79, 225–229.

[44] Ho, S. N., Hunt, H. D., Horton, R. M., Pullen, J. K., Pease, L. R. (1989) Gene 77, 51–59.
[45] Brewer, J. A., Sleckman, B. P., Swat, W., Muglia, L. J. (2002) J. Immunol. 169, 1309–1318.
[46] Bradford, M. M. (1976) Anal. Biochem. 72, 248–254.
[47] Laemmli, U. K. (1970) Nature 227, 680–685.
[48] Guo, H. B., Johs, A., Parks, J. M., Olliff, L., Miller, S. M., Summers, A. O., Liang, L., Smith, J. C. (2010) J. Mol. Biol. 398, 555–568.
[49] Yang, J., Zhang, Y. (2015) Curr. Protoc. Bioinformatics 52, 5.8.1-5.8.15.
[50] Ralston, D. M., O'Halloran, T. V. (1990) Proc. Natl. Acad. Sci. USA 87, 3846–3850.
[51] Thirupathi, P., Lee, K. H. (2013) Bioorg. Med. Chem. 21, 7964–7970.
[52] Siepi, M., Oliva, R., Petraccone, L., Del Vecchio, P., Ricca, E., Isticato, R., Notomista, E., Donadio, G. (2018) PLoS One 13, e0204164.
[53] Nadarajan, S. P., Ravikumar, Y., Deepankumar, K., Lee, C. S., Yun, H. (2014). Chem. Commun. 50, 15979–15982.
[54] Tainaka, K., Sakaguchi, R., Hayashi, H., Nakano, S., Liew, F. F., Morii, T. (2010). Sensors 10, 1355–1376.
[55] Hu, H., Gu, Y., Xu, L., Zou, Y., Wang, A., Tao, R., Chen, X., Zhao, Y., Yang, Y. (2017). Sci. Rep. 7, 43479.
[56] Isarankura-Na-Ayudhya, C., Tantimongcolwat, T., Galla, H. J., Prachayasittikul, V. (2010). Biol. Trace Elem. Res. 134, 352–363.
[57] Sundberg, R. J., Martin, R. B. (1974). Chem. Rev. 74, 471–517.
[58] Carrera, F., Marcos, E. S., Merkling, P. J., Chaboy, J., Munoz-Páez, A. (2004). Inorg. Chem. 43, 6674–6683.
[59] Wątły, J., Hecel, A., Rowińska-Żyrek, M., Kozłowski, H. (2018). Inorg. Chim. Acta 472, 119–126.
[60] Roointan, A., Shabab, N., Karimi, J., Rahmani, A., Alikhani, M. Y., Saidijam, M. (2015). Turk. J. Biol. 39, 550–555.
[61] Janczak, M., Bukowski, M., Górecki, A., Dubin, G., Dubin, A., Wladyka, B. (2015). Acta Biochim. Pol. 62, 407–411.